UWBOri: Enabling Accurate Orientation Estimation with Ultra-wideband Signals

Zhaoxin Chang, Fusang Zhang, Jie Xiong, Xinyu Xue, Zeyu Wang, Badii Jouaber, Daqing Zhang

UWBOri: Enabling Accurate Orientation Estimation with Ultra-wideband Signals

Zhaoxin Chang[1], Fusang Zhang[2], Jie Xiong[3], Xinyu Xue[1], Zeyu Wang[4], Badii Jouaber[1], Daqing Zhang[1,5]
[1]SAMOVAR, Telecom SudParis, Institut Polytechnique de Paris,
[2]Institute of Software, Chinese Academy of Sciences and University of Chinese Academy of Sciences,
[3]Microsoft Research Asia and University of Massachusetts Amherst,
[4]University of Michigan, Ann Arbor, [5]Peking University

***Abstract*—The development of smart devices has highlighted the need for human-device interaction. A key aspect of this interaction lies in the estimation of the physical orientation of the device, which is crucial for various applications. Conventional methods employing Inertial Measurement Units (IMU) encounter limitations such as cumulative errors and magnetic interference. In this paper, we propose UWBOri, a novel method for orientation estimation using Ultra-wideband (UWB) technology. UWB technology, which is increasingly integrated into smart devices, offers superior ranging accuracy owing to its large bandwidth. By leveraging the localization information obtained between a fixed UWB-equipped anchor device and the user device, UWBOri can accurately estimate the orientation of the user device. The efficacy of UWBOri has been validated through extensive laboratory experiments designed to evaluate the accuracy of orientation estimation. Furthermore, we demonstrate the practical applicability of UWBOri in two distinct scenarios: IoT device selection and augmented reality (AR). These applications illustrate the potential of our solution in real-world scenarios.**

***Index Terms*—Orientation, Ultra-wideband, Smart devices, Human-device interaction**

I. Introduction

Recent years have witnessed the rapid development of smart devices, including smartphones, smartwatches, earphones, and smart glasses. A growing focus is on improving human-device interaction to create innovative and practical applications. To achieve efficient interaction, it is often necessary to determine the physical state of a smart device, including its location and orientation. While localization has been extensively studied, research on orientation estimation for smart devices remains relatively limited. However, orientation estimation is critically important as it supports numerous applications. For instance, in AR applications, accurate orientation allows users to interact seamlessly with virtual objects overlayed in the real world. Knowing the device's orientation improves directional guidance and spatial awareness in precise navigation. Accurate orientation information can significantly enhance the user experience and extend the functionality and usability of smart devices in various complex scenarios.

On smart devices such as smartphones, conventional orientation estimation typically relies on IMUs. Within the IMU, the gyroscope and the magnetometer are commonly used for orientation estimation. However, gyroscopes often face the issue of cumulative errors, leading to drift over time. On the other hand, magnetometers can be affected by magnetic interference from components in commercial devices, resulting in inaccurate measurements [1]. To this end, researchers have also proposed installing various wireless signal modules on devices for orientation estimation, including RFID [2], [3], Wi-Fi [4], LoRa [5], Bluetooth [6], and acoustic signals [1], [7]. By analyzing the signals received or transmitted by the antennas at different locations on the device, the orientation of the device can be inferred. However, these signals are either unavailable on commercial smart devices or difficult to extract the channel state information needed for orientation estimation. Therefore, achieving precise and reliable orientation estimation in commercial devices remains a challenge.

In this paper, we propose a novel orientation estimation method for smart devices utilizing UWB technology. Currently, UWB technology is being widely deployed in various smart devices, including smartphones, smartwatches, and smart speakers. Due to its larger bandwidth (i.e., 500 MHz) compared to other Radio Frequency (RF) signals, UWB offers superior ranging accuracy. Additionally, when combined with multi-antenna technology, the Angle-of-Arrival (AoA) of UWB signal can also be estimated. Therefore, UWB is highly suitable for device localization. For example, a UWB-equipped iPhone can locate an AirTag attached to an item, facilitating item tracking [8].

In this paper, we further explore the application of UWB's localization capabilities to facilitate orientation estimation. Specifically, our core idea is that, given the fixed locations of two UWB-enabled devices (denoted as devices A and B), when the orientation of device A changes, the relative location of device B with respect to device A also changes. Therefore, the localization data inherently incorporates orientation information. With this key insight, we propose UWBOri, a UWB-based orientation estimation method. First, one UWB-equipped device (e.g., a smart speaker or a smart TV) is fixed in the environment as an anchor. Subsequently, leveraging the UWB connection between the anchor and the user's smart device (e.g., a smartphone) and the corresponding localization information reported, we can accurately estimate the orientation of the user's device.

We implement UWBOri on UWB-equipped iPhones. To validate the effectiveness of the proposed orientation estimation

Corresponding Authors: Daqing Zhang and Fusang Zhang

approach, we conduct comprehensive benchmark experiments in laboratory scenarios. Then, we demonstrate the application of UWBOri in two real-world scenarios, including IoT device selection and AR.

The main contributions of this work are summarized as follows:

- We present a novel orientation estimation solution using UWB-equipped smart devices.
- We prototype the proposed method based on commodity smartphones.
- We validate the effectiveness of our method in laboratory settings and demonstrate its potential through practical applications in real-world environments.

II. Preliminary

In this section, we first present the background knowledge of UWB and then introduce the definition of orientation.

A. Background of UWB

The typical characteristic of UWB signals is their large bandwidth. In the time domain, UWB signals appear as very short pulses. The bandwidth of UWB signals transmitted by commercial devices is typically 500 MHz, which corresponds to a pulse duration of 2 ns [9]. Therefore, the direct path signal between two devices can be distinguished from multipath signals in the time domain, enabling precise measurement of the signal's Time-of-Flight (ToF). Furthermore, using Two Way Ranging (TWR) [10], [11] algorithms, the distance between two devices can be estimated. Meanwhile, if the UWB receiver is equipped with multiple antennas, the AoA of the received signal can be estimated by measuring the phase differences between signals received by different antennas [12]. Finally, by combining distance and angle information, the relative location coordinates between devices can be calculated.

In recent years, more and more manufacturers have included UWB modules in their smart devices (e.g., smartphones, smartwatches, smart speakers, earphones, and TVs) for localization, including Apple [13], Samsung [14], Xiaomi [15] and Google [16]. In this paper, we use the UWB-equipped iPhone (i.e., iPhone 11 and later) as the platform to implement the proposed orientation estimation method. Using the Nearby Interaction API [13] provided by Apple, UWB connections can be established between iPhone devices. After its establishment, each smartphone can measure and report the distance and angle of other devices relative to itself, enabling device localization.

B. Definition of Orientation

For simplicity, in this paper, we assume the user's smart device is a smartphone. First, we define a smartphone coordinate system (C_s) that is bound to the smartphone. As shown in Figure 1a, the x-axis and z-axis of C_s are parallel to the two sides of the smartphone respectively, and the y-axis is perpendicular to the smartphone surface. Then, we define a base coordinate system (C_a), which can be established with a fixed point in the environment as the origin. As shown in Figure 1b, we define the orientation of the smartphone as the direction of the y-axis of C_s, which can be represented as a unit vector $n_{ori} = (e_x, e_y, e_z)^T$ in C_a. Based on this definition, we present the principle of orientation estimation and the system prototype.

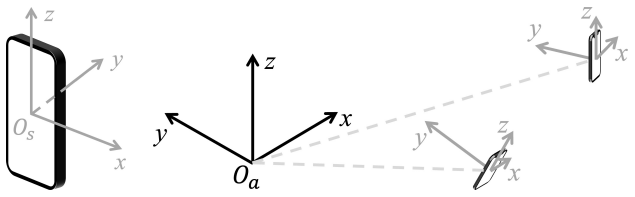

(a) Smartphone coordinate system.

(b) Illustration of smartphone orientation.

Fig. 1: The definition of smartphone orientation. The orientation of a smartphone is determined by its y-axis direction in the base coordinate system.

III. Principle of Orientation Estimation

In this section, we propose the detailed principle of orientation estimation. As introduced in Section II-B, the orientation of the smartphone is defined as the direction vector (n_{ori}) of the y-axis of the smartphone coordinate system C_s and the y-axis is perpendicular to the smartphone surface. Traditional orientation estimation approaches on smart devices are based on sensors such as accelerometers and magnetometers [17], [18]. However, magnetic fields from ferromagnetic objects in the indoor environment and ferromagnetic components inside the smartphone can interfere with the measurement of the magnetometer, resulting in inaccurate orientation estimation [1]. In this paper, we estimate the orientation only based on the UWB readings, which are more resistant to interference.

As introduced in Section II-A, UWB technology is dedicated to device localization. To this end, a UWB-equipped anchor is required to be fixed in the environment. In this paper, we use an iPhone as an anchor to validate and prototype our method. Note that in real-world deployments, this anchor could be a smart device (such as a smart speaker or a smart TV) or a dedicated UWB device. The key observation behind our solution is, when the user device and anchor have different orientations, the angle of the user device with respect to the anchor is always different from the angle of the anchor with respect to the user device. This angle difference also induces different location estimation results for the user device and anchor, i.e. the location of the user device estimated by the anchor is different from the location of the anchor estimated by the user device.

As shown in Figure 2a, we define the base coordinate system (C_a) which is bound to the anchor. When the orientation of the user device changes, the locations of the anchor in C_s (user device's view) are different. Let $p_a = (x_a, y_a, z_a)^T$ denote the location of the anchor in the view of the user device (C_s). It is intuitive that the locations of the anchor in the view of the user

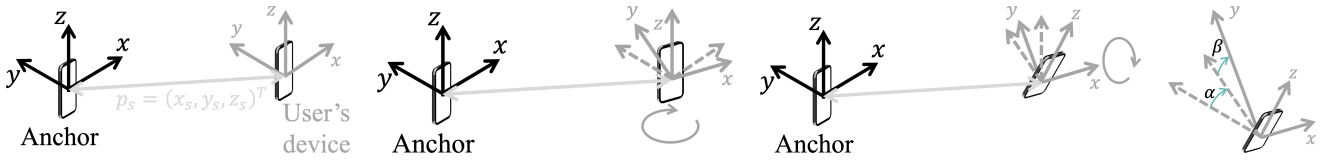

(a) Illustration of the initial orientation. (b) Rotating around the z-axis. (c) Rotating around the x-axis. (d) Illustration of user device's orientation.

Fig. 2: Illustration of orientation estimation. The orientation of the user device can be represented as obtained by rotating the initial orientation by α around the z-axis and β around the x-axis in sequence.

device can be used to infer its orientation. We first define an initial orientation, which is the same as the orientation of the anchor as shown in Figure 2a. In the initial state, the axes of C_s are parallel to that of C_a. Note that the location of user device in C_a is $p_s = (x_s, y_s, z_s)^T$. Thus, the location of anchor in C_s is $p_{a0} = (-x_s, -y_s, -z_s)^T$ and the initial orientation vector is $n_0 = (0, 1, 0)^T$. Then, the user device can be rotated to different orientations. As shown in Figure 2b, the user device can rotate around the z-axis. Furthermore, it can rotate around the x-axis as shown in Figure 2c. The angle of rotation around z-axis and x-axis is denoted as azimuth angle α and elevation angle β, respectively. Thus, any orientation can be expressed by rotating the initial orientation by α around z-axis and β around x-axis as shown in Figure 2d. Note that for the initial virtual and true orientation, the locations of the anchor in the view of the user device are p_{a0} and p_a, respectively. We can use a rotation matrix, M_R, to characterize the transformation of the location of the anchor from the initial virtual orientation to real orientation [19]:

$$\begin{aligned} M_R &= M_x M_z \\ &= \begin{pmatrix} 1 & 0 & 0 \\ 0 & \cos\beta & -\sin\beta \\ 0 & \sin\beta & \cos\beta \end{pmatrix} \begin{pmatrix} \cos\alpha & -\sin\alpha & 0 \\ \sin\alpha & \cos\alpha & 0 \\ 0 & 0 & 1 \end{pmatrix}, \end{aligned} \tag{1}$$

where M_x and M_z are the rotation matrices around x-axis and z-axis, respectively. Note that the initial orientation is a virtual orientation indicating the user device is facing the same orientation as the anchor. Then, the transformation relationship between the anchor location before and after the user device's rotation can be expressed as:

$$p_a = M_R p_{a0} = M_x M_z p_{a0}. \tag{2}$$

Then, the azimuth angle (α) and elevation angle (β) can be calculated as:

$$\beta = \begin{cases} \arccos\dfrac{-z_s}{d} + \arctan\dfrac{y_a}{z_a} & , \text{ if } z_a < 0 \\ \arccos\dfrac{-z_s}{d} + \arctan\dfrac{y_a}{z_a} - \pi & , \text{ if } z_a \geq 0 \end{cases} \tag{3}$$

$$\alpha = \arctan\frac{x_a y_s - A x_s}{x_a x_s + A y_s}, A = y_a \cos\beta - z_a \sin\beta.$$

Consequently, the orientation vector of the user device (i.e., the direction of the y-axis) can be obtained as below:

$$n_{ori} = (cos\alpha cos\beta, cos\alpha sin\beta, sin\alpha)^T. \tag{4}$$

Thus, for orientation estimation, we rely solely on the location of the user device as measured by the anchor, and the location of the anchor as measured by the user device.

IV. Implementation

In this paper, we implement our design based on Apple products. Specifically, we employ an iPhone 11 as a fixed anchor in the test environment, while an iPhone 12 Pro Max is used for orientation estimation. To facilitate our design, we build an iOS application leveraging Nearby Interaction framework [13], which enables the establishment of a pear-to-pear UWB connection between the two iPhones. Then, both smartphones are able to measure the distance and angle of the other, resulting in the acquisition of UWB measurements from both sides. To evaluate our design, we export the collected data from two smartphones to a server laptop (a MacBook Pro with an Intel Core i7 CPU and 32GM RAM) via a UDP connection. It is worth noting that Android also provides UWB measurement collection API for devices [20]. Meanwhile, Apple devices possess the capability to establish a UWB connection with third-party UWB-equipped hardware [21]. This implies that our design has the potential to be implemented on a broader range of devices.

V. Evaluation

In this section, we first conduct benchmark experiments in laboratory environments to evaluate the performance of orientation estimation. Then, we present two real-world application scenarios in which our proposed method can be employed, including IoT device selection and AR.

A. Evaluation of Orientation Estimation

In this section, we conduct benchmark experiments to evaluate the performance of orientation estimation.

1) Experiment Setting: We evaluate the accuracy of the orientation estimation across different smartphone positions. We move the smartphone away from the anchor from 1 m to 5 m at a step of 1 m. At a distance of 3 m, we move the smartphone from $-40°$ to $40°$ at a step of $20°$. In each position, we vary the orientation of the smartphone from $-50°$ to $50°$ at a step of $10°$ for both azimuth and elevation angles. We calculate the mean absolute error (MAE) between the estimated value and ground truth. We also compare the results estimated by our method with those by IMU readings.

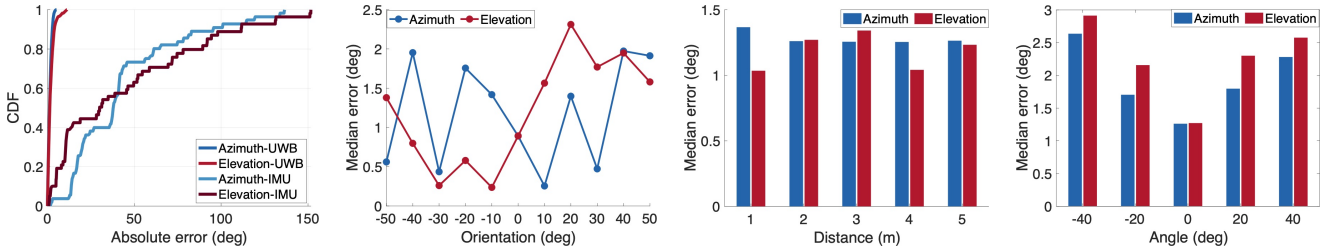

(a) Overall performance. (b) Different orientations. (c) Different distances. (d) Different angles.

Fig. 3: Performance of orientation estimation.

2) Overall Performance: Figure 3a shows the overall orientation estimation errors using our design and IMU-based solutions. The median error of our design is $1.52°$ and $1.48°$ for azimuth angle and elevation angle, respectively, while that of IMU-based solution is $41.2°$ and $46.8°$. This result shows that our design significantly outperforms the method based on IMU data on the smartphone. Figure 3b shows the estimation error for different orientations. For all orientations, the estimation errors are below $2.4°$.

3) Impact of Distance and Angle between the User Device and Anchor: Figures 3c and 3d show the impact of distance and angle between the smartphone and the anchor. We can observe that for all distances between the user's smartphone and the anchor, the median orientation error is lower than $1.4°$. We also find that the orientation error slightly increases with the angle of the user's smartphone with respect to the anchor. When the angle of the smartphone is $-40°$, the median orientation error reaches a maximum value of $2.6°$ and $2.8°$ which are still small enough for azimuth angle and elevation angle, respectively. These results show that our design can achieve a high orientation estimation accuracy.

B. Application 1: IoT Device Selection

In smart homes, an increasing number of appliances can be connected to the network. How to efficiently enable users to select the device they want to control is a crucial factor affecting the user experience. Traditional methods involve selecting from a list on a smartphone or using a voice assistant. Our proposed orientation estimation method provides a new and simple way for IoT device selection. Regardless of the user's location, they can select the device they want to control simply by pointing their smartphone at it. To achieve this, it is necessary to know the location and orientation of the user's smartphone. The location can be measured directly by the anchor, and the orientation can be estimated using our method based on the location information. Based on the location and orientation of the smartphone, the pointing direction of the user can be obtained as a line equation:

$$p = p_s + k \cdot n_{ori}, \tag{5}$$

where p represents the points in the pointing direction and k is the variable parameter of the line equation. Subsequently, the selected device can be identified by determining whether each IoT device lies in the direction the smartphone is pointing.

1) Experiment Setting: We first validate the concept and evaluate the performance of pointing direction estimation in a laboratory environment. As shown in Figure 4a, we place nine points on a wall. The distance between adjacent points is 1 m. The anchor is next to the point in the middle of the left column. We recruit six participants to hold the smartphone and point at all points at different distances, angles, and heights. The estimation error is calculated as the shortest distance between this point and the pointing direction of the smartphone.

2) Impact of Distance: Figure 4b shows the pointing direction estimation errors under different distances between the anchor and user smartphone. When the distance from the smartphone to the anchor is 2 m, 3 m, 4 m, and 5 m, the median values of the errors (including all nine points) are 0.06 m, 0.10 m, 0.16 m, and 0.25 m, respectively. Figure 4e to 4h show the errors when pointing to the nine points respectively. The accuracy of pointing direction estimation decreases with the increase of distance between the anchor and target point. When the distance between the wall and smartphone is 5 m, the system reaches a maximum error of 0.314 m. Considering the typical size of a room, placing the anchor at the center position of a wall can ensure sufficient pointing direction estimation accuracy of all the IoT devices in the room.

3) Impact of Angle: Figure 4c shows the CDF plot of pointing direction estimation errors at different angles. When the angle varies from $0°$ to $40°$, the average error is slightly increases by 0.06 m, indicating a small effect of the smartphone angle on the performance.

4) Impact of Height: Figure 4d shows the CDF errors at three smartphone heights (i.e., 0.5 m, 1 m, and 1.5 m). The pointing direction estimation errors at these three heights are 0.14 m, 0.11 m, and 0.09 m, respectively. These results show that our system can achieve good performance for different user body postures such as lying (i.e., 0.5 m), sitting (i.e., 1.0 m), and standing (i.e., 1.5 m).

5) Impact of Anchor Location: In this experiment, we evaluate the impact of anchor location on pointing direction estimation. In the experiment setting (Figure 4a), we change the location of the anchor in two dimensions. First, starting from the anchor location shown in the figure, we change the

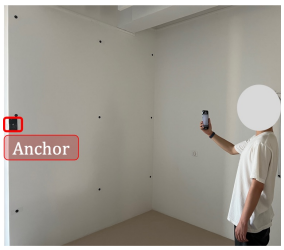

(a) Experiment setting.

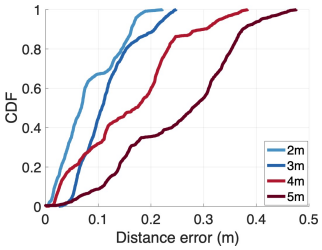

(b) Smartphone at different distances.

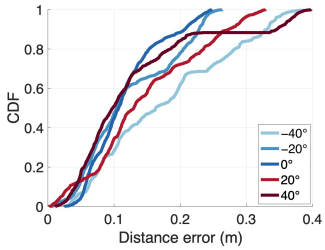

(c) Smartphone at different angles.

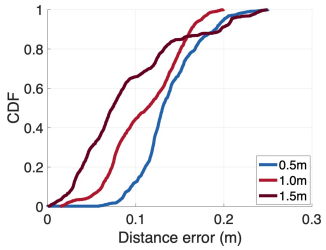

(d) Smartphone at different heights.

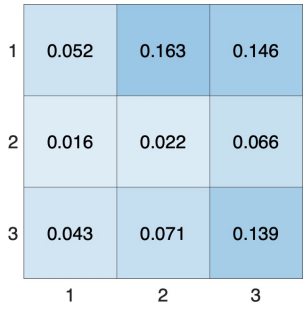

(e) At a distance of 2 m.

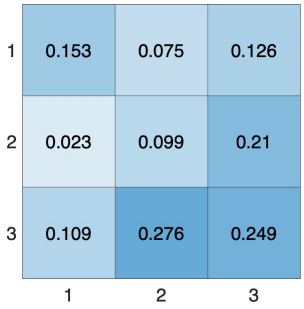

(f) At a distance of 3 m.

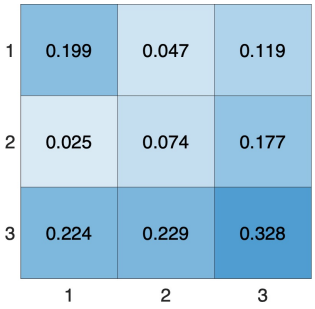

(g) At a distance of 4 m.

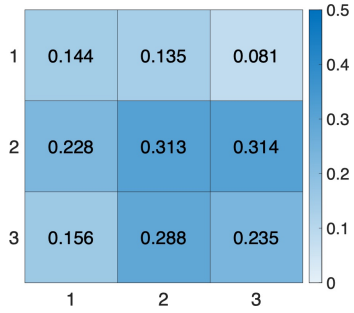

(h) At a distance of 5 m.

Fig. 4: Accuracy of pointing direction estimation.

distance of the anchor to the wall from 0 m to 2 m at a step of 0.5 m. Then, starting from the center point in the figure, we move the anchor to the left from 0 m to 2 m at a step of 0.5 m. During this experiment, the distance between the wall and the person is 4 m. Figure 5a and 5b show the pointing direction estimation error with different anchor locations. As the distance between the anchor and the wall increases, the pointing direction estimation error decreases. This is because when the distance between the anchor and user smartphone becomes closer, the angle estimation error declines. As the distance between the anchor and the center point increases, the estimation error also increases. This is due to the angle of anchor measured by the user smartphone and the angle of user smartphone measured by the anchor increases, resulting in a larger angle and orientation estimation error.

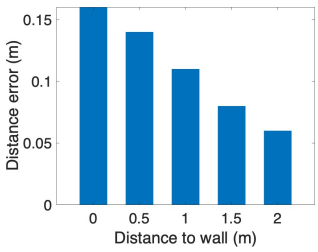

(a) Impact of the distance between anchor and wall.

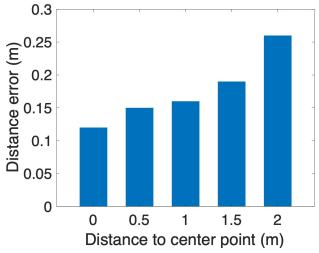

(b) Impact of the distance between anchor and center point.

Fig. 5: Impact of anchor location.

6) Evaluation in Real-world Environments: In this section, we evaluate our system in four real-world environments shown in Figure 6. The first environment is a small bedroom with a size of 2.7 $m \times 5$ m. There are eight devices in the bedroom, including two lamps (D1 and D8), a humidifier (D2), a monitor (D3), a curtain (D4), a window (D5), a heater (D6) and a router (D7). The second environment is a large bedroom with a size of 4.3 $m \times 6.5$ m. There are nine devices in the bedroom, including a window (D1), a curtain (D2), three lamps (D3, D4 and D7), a TV (D5), an air purifier (D6), an air conditioner (D8) and a refrigerator (D9). The third environment is a meeting room with a size of 2.5 $m \times 3$ m.

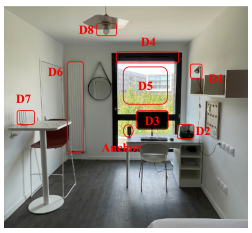

(a) A small bedroom.

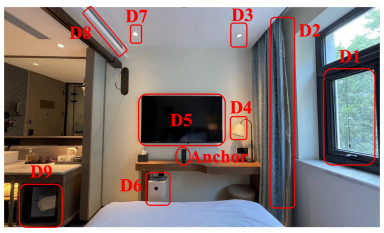

(b) A large bedroom.

(c) A meeting room.

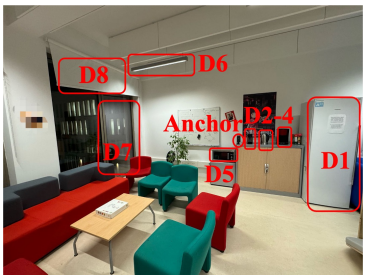

(d) A lounge.

Fig. 6: Four real-world environments.

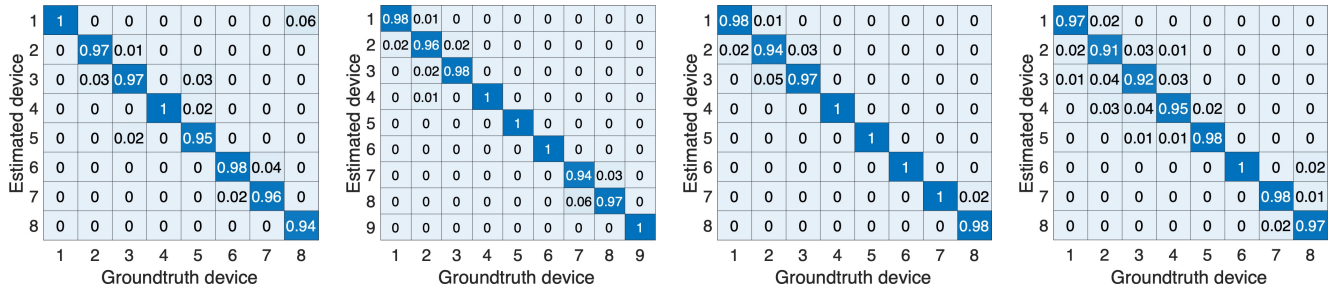

(a) A small bedroom. (b) A large bedroom. (c) A meeting room. (d) A lounge.

Fig. 7: Confusion matrices of IoT device selection.

There are eight devices in the meeting room, including an air conditioner (D1), a light (D2), a ventilation fan (D3), a TV (D4), a router (D5), a smart speaker (D6), a window (D7) and a curtain (D8). The fourth environment is a lounge with a size of 3 $m \times 3.5$ m. There are eight devices in the lounge, including a refrigerator (D1), three coffee machines (D2 and D4), a kettle (D3), a microwave oven (D5), a light (D6), a window (D7) and a curtain (D8). In each environment, we recruit six participants to point at all devices at ten different locations. At each location, each participant points at each device five times.

Figure 7 shows the confusion matrices of device selection in each environment. The average accuracy of device selection in four scenarios is 97.1%, 98.1%, 98.4%, and 96.0% respectively. We further analyze the cases of incorrect selection. The reason for wrong selection is mainly due to the close proximity of IoT devices. Take D6 and D7 in S1 as an example. As shown in Figure 6a, when pointing at D7 near the left wall of the room, D6 is also close to the direction the smartphone is pointing at. This shows that when pointing at one IoT device, the user is suggested to make sure other devices are not in the direction the smartphone is pointing at.

C. Application 2: AR Scenarios

In this section, we demonstrate the potential of our design in AR scenarios in two real-world environments. In environments such as a museum, an AR app on the mobile device can help improve user experience and provide innovative ways to interact with the surroundings [22], [23]. For example, when a person enters a museum and wishes to find a certain exhibit or preview the exhibits in a room, she/he can take out the smartphone and point it at each exhibit. The AR app can display the information of each exhibit on the screen, thereby helping users quickly find the location of her/his interests. We demonstrate the feasibility of our design for an AR app in a museum environment with a size of 3 $m \times 7$ m and a conference environment with a size of 2.5 $m \times 6$ m as shown in Figure 8. There are 9 objects in each environment. When the user picks up the smartphone and points it at an object, our method is used to identify it. We point at all objects at ten different locations. Results show that the accuracy of object selection in two environments is 95.2% and 96.8%, respectively.

(a) A museum environment. (b) A conference environment.

Fig. 8: Application in AR scenarios.

VI. Related Work

In this section, we discuss the most related literature.

A. Orientation Estimation

With the rapid development of smart devices, accurate orientation estimation has become essential for various applications. Researchers have explored multiple approaches for orientation estimation. Conventional orientation estimation relies on the IMU, which faces challenges such as cumulative drift errors and magnetic interference. Traditional filtering methods [24], [18] and deep learning techniques [25], [26] have been explored to address these issues. However, even with advanced deep learning methods, orientation estimation errors remain at a minimum of 4.6° [26]. In recent years, researchers have explored orientation estimation based on various wireless signals, including RFID [2], [3], Wi-Fi [4], LoRa [5], Bluetooth [6], and acoustic signals [7], [1]. For example, LoRa backscatter tags have been placed on drones for orientation detection [5]. BLESelect [6] estimates the orientation of smart glasses by installing multi-antenna BLE devices. FaceOri [7] measures the distance difference between microphones on an earphone and a speaker to determine the earphone's orientation. However, RFID and LoRa are not available on most commercial smart devices. Wi-Fi and BLE on commercial devices are primarily used for communication, making it difficult to extract the raw signals needed for

orientation estimation. Acoustic signals have a short working range and are easily interfered. In this paper, we propose using UWB signals for orientation estimation. UWB has already been widely deployed in commercial devices and can provide the necessary positioning information for accurate orientation estimation.

B. UWB Techniques

UWB technology utilizes large bandwidth pulses as the baseband signal, making precise device positioning possible [27], [28]. This has led to numerous positioning-related applications, including tracking [29], [30], item finding [8], [31], digital keys [32], and handwriting recognition [33], [34]. By analyzing the propagation of UWB signals in space, it can also be used for contactless sensing, such as monitoring respiration [35], [36], heartbeat [37], [38], and blood pressure [39].

VII. Discussion

A. System Generalization

1) Generalization Across Smart devices: In this paper, we implement our system using iPhones due to the availability of detailed UWB reading extraction APIs provided by Apple for all UWB-equipped iPhones. We also observed a growing trend in the integration of UWB technology in Android smartphones. As of June 2023, the Android 12 API includes the UWB API [20] that supports UWB data extraction from Samsung and Google Pixel phones. Recent work [12] compares the accuracy of UWB data extracted from various smartphone models, and the results indicate similar levels of accuracy. Consequently, our system can be extended to Android devices that support UWB data extraction. Looking ahead, we expect that more Android smartphones will incorporate UWB technology, enabling the application of our design on a wide range of smartphones. We also observe that more and more smartwatches are equipped with UWB. At the same time, we envision that more smart devices will be equipped with UWB in the future, allowing our technology to be used in more scenarios.

2) Implementation of UWB Anchor: In this paper, we utilize an iPhone 11 as the fixed UWB anchor in the environment. For real-world deployment, we envision two alternatives for the anchor. Firstly, the anchor can be realized by utilizing UWB-equipped smart devices. For example, smart speakers and TVs produced by Apple and Xiaomi have integrated UWB modules. Currently, these manufacturers have not released the UWB data collection API for these smart devices. Alternatively, the UWB anchor can be implemented by leveraging third-party UWB chips and development boards [40], [41]. These third-party UWB products can establish UWB connections with commercial smartphones and support data extraction, enabling our system design.

B. System Extension

In Section V-C, we present an example application of our system. In AR/VR scenarios, accurate estimation of orientation and pointing direction serves as a fundamental requirement for various applications. Our method offers a solution for estimating the orientation and pointing direction of devices, thus providing essential information for a wide range of AR/VR applications. Compared to existing pointing direction estimation technologies in AR/VR, our design offers a notable advantage by seamlessly combining the device's pointing direction with the actual position of objects in the physical space, resulting in an enhanced interactive experience. By implementing orientation and pointing direction estimation on smartphones and wearable devices, our method can support a large range of other applications including activity and gesture recognition [7] and 3D reconstruction [1].

VIII. Conclusion

In this paper, we present a novel design for estimating the orientation of smart devices using UWB technology. The key innovation of our design lies in leveraging localization information to infer orientation. To validate our system, we conduct comprehensive evaluations in both controlled lab settings and real-world environments. The results demonstrate the promising potential of the proposed system for real-world deployment. We believe that our technology can benefit a wide range of AR/VR/HCI applications.

Acknowledgments

This work is partially supported by the European Union through the Horizon EIC pathfinder challenge project SUSTAIN (No. 101071179), the Innovative Medicines Initiative 2 Joint Undertaking project IDEA-FAST (No. 853981), the National Natural Science Foundation of China (No.62172394 and No. 62422213), and the Beijing Natural Science Foundation (L223034), Innovation Team 2024 ISCAS (No. 2024-66), and the Beijing Nova Program.

References

[1] Z. Gao, A. Li, D. Li, J. Liu, J. Xiong, Y. Wang, B. Li, and Y. Chen, "Mom: Microphone based 3d orientation measurement," in *2022 21st ACM/IEEE International Conference on Information Processing in Sensor Networks (IPSN)*. IEEE, 2022, pp. 132–144.

[2] L. Shangguan and K. Jamieson, "Leveraging electromagnetic polarization in a two-antenna whiteboard in the air," in *Proceedings of the 12th International on Conference on emerging Networking EXperiments and Technologies*, 2016, pp. 443–456.

[3] T. Wei and X. Zhang, "Gyro in the air: tracking 3d orientation of batteryless internet-of-things," in *Proceedings of the 22nd Annual International Conference on Mobile Computing and Networking*, 2016, pp. 55–68.

[4] C. Wu, F. Zhang, Y. Fan, and K. R. Liu, "Rf-based inertial measurement," in *Proceedings of the ACM Special Interest Group on Data Communication*, 2019, pp. 117–129.

[5] S. Zhang, W. Wang, N. Zhang, and T. Jiang, "Lora backscatter assisted state estimator for micro aerial vehicles with online initialization," *IEEE Transactions on Mobile Computing*, vol. 21, no. 11, pp. 4038–4050, 2021.

[6] T. Zhang, Z. Lan, C. Xu, Y. Li, and Y. Chen, "Bleselect: Gestural iot device selection via bluetooth angle of arrival estimation from smart glasses," *Proceedings of the ACM on Interactive, Mobile, Wearable and Ubiquitous Technologies*, vol. 6, no. 4, pp. 1–28, 2023.

[7] Y. Wang, J. Ding, I. Chatterjee, F. Salemi Parizi, Y. Zhuang, Y. Yan, S. Patel, and Y. Shi, "Faceori: Tracking head position and orientation using ultrasonic ranging on earphones," in *Proceedings of the 2022 CHI Conference on Human Factors in Computing Systems*, 2022, pp. 1–12.

[8] (2021) Find your keys, wallet, and more with airtag. [Online]. Available: https://support.apple.com/en-us/HT210967

[9] F. Sabath, E. Mokole, and S. Samaddar, "Definition and classification of ultra-wideband signals and devices," *URSI Radio Science Bulletin*, vol. 2005, no. 313, pp. 12–26, 2005.

[10] M. P. Layer, "Part 15.4: Low-rate wireless personal area networks (lr-wpans)," 2013.

[11] D. Neirynck, E. Luk, and M. McLaughlin, "An alternative double-sided two-way ranging method," in *2016 13th workshop on positioning, navigation and communications (WPNC)*. IEEE, 2016, pp. 1–4.

[12] A. Heinrich, S. Krollmann, F. Putz, and M. Hollick, "Smartphones with uwb: Evaluating the accuracy and reliability of uwb ranging," *arXiv preprint arXiv:2303.11220*, 2023.

[13] (2023) Nearby interaction. [Online]. Available: https://developer.apple.com/documentation/nearbyinteraction

[14] (2021) What is ultra-wideband (uwb) technology on samsung phones? how is it helpful? [Online]. Available: https://www.smartprix.com/bytes/phones-with-uwb-ultrawideband-connectivity/

[15] (2020) Xiaomi introduces groundbreaking uwb technology. [Online]. Available: https://blog.mi.com/en/2020/10/13/xiaomi-introduces-groundbreaking-uwb-technology/

[16] (2021) Google reiterates that pixel 6 will have uwb as it works to expand support in android 13. [Online]. Available: https://9to5google.com/2021/08/25/google-pixel-6-uwb-mention/

[17] P. Zhou, M. Li, and G. Shen, "Use it free: Instantly knowing your phone attitude," in *Proceedings of the 20th annual international conference on Mobile computing and networking*, 2014, pp. 605–616.

[18] S. Shen, M. Gowda, and R. Roy Choudhury, "Closing the gaps in inertial motion tracking," in *Proceedings of the 24th Annual International Conference on Mobile Computing and Networking*, 2018, pp. 429–444.

[19] D. Q. Huynh, "Metrics for 3d rotations: Comparison and analysis," *Journal of Mathematical Imaging and Vision*, vol. 35, pp. 155–164, 2009.

[20] (2023) Ultra-wideband (uwb) communication. [Online]. Available: https://developer.android.com/guide/topics/connectivity/uwb

[21] (2022) Nearby interaction with uwb. [Online]. Available: https://developer.apple.com/nearby-interaction/

[22] Z. Gong, R. Wang, and G. Xia, "Augmented reality (ar) as a tool for engaging museum experience: a case study on chinese art pieces," *Digital*, vol. 2, no. 1, pp. 33–45, 2022.

[23] J. Hahn, "Mobile augmented reality applications for library services," *New library world*, vol. 113, no. 9/10, pp. 429–438, 2012.

[24] S. O. Madgwick, A. J. Harrison, and R. Vaidyanathan, "Estimation of imu and marg orientation using a gradient descent algorithm," in *2011 IEEE international conference on rehabilitation robotics*. Ieee, 2011, pp. 1–7.

[25] M. A. Esfahani, H. Wang, K. Wu, and S. Yuan, "Orinet: Robust 3-d orientation estimation with a single particular imu," *IEEE Robotics and Automation Letters*, vol. 5, no. 2, pp. 399–406, 2019.

[26] S. Sun, D. Melamed, and K. Kitani, "Idol: Inertial deep orientation-estimation and localization," in *Proceedings of the AAAI Conference on Artificial Intelligence*, vol. 35, no. 7, 2021, pp. 6128–6137.

[27] W. C. Chung and D. Ha, "An accurate ultra wideband (uwb) ranging for precision asset location," in *IEEE Conference on Ultra Wideband Systems and Technologies, 2003*. IEEE, 2003, pp. 389–393.

[28] J. Ma, F. Zhang, B. Jin, C. Su, S. Li, Z. Wang, and J. Ni, "Push the limit of highly accurate ranging on commercial uwb devices," *Proceedings of the ACM on Interactive, Mobile, Wearable and Ubiquitous Technologies*, vol. 8, no. 2, pp. 1–27, 2024.

[29] J. Yang, B. Dong, and J. Wang, "Vuloc: Accurate uwb localization for countless targets without synchronization," *Proceedings of the ACM on Interactive, Mobile, Wearable and Ubiquitous Technologies*, vol. 6, no. 3, pp. 1–25, 2022.

[30] Y. Zhou, C. L. Law, and J. Xia, "Ultra low-power uwb-rfid system for precise location-aware applications," in *2012 IEEE Wireless Communications and Networking Conference Workshops (WCNCW)*. IEEE, 2012, pp. 154–158.

[31] Z. Wang, S. Li, Z. Zhang, F. Lv, and Y. Hou, "Research on uwb positioning accuracy in warehouse environment," *Procedia computer science*, vol. 131, pp. 946–951, 2018.

[32] Z. Zheng, S. Yan, L. Sun, H. Shu, and X. Zhou, "Nn-lcs: Neural network and linear coordinate solver fusion method for uwb localization in car keyless entry system," *Sensors*, vol. 23, no. 5, p. 2694, 2023.

[33] J. Ma, Z. Chang, F. Zhang, J. Xiong, J. Ni, B. Jin, and D. Zhang, "Involving ultra-wideband in consumer-level devices into the ecosystem of wireless sensing," in *Proceedings of the 28th Annual International Conference on Mobile Computing And Networking*, 2022, pp. 758–760.

[34] Y. Cao, A. Dhekne, and M. Ammar, "Utrack3d: 3d tracking using ultra-wideband (uwb) radios," in *Proceedings of the 22nd Annual International Conference on Mobile Systems, Applications and Services*, 2024, pp. 345–358.

[35] F. Zhang, J. Xiong, Z. Chang, J. Ma, and D. Zhang, "Mobi2sense: empowering wireless sensing with mobility," in *Proceedings of the 28th Annual International Conference on Mobile Computing And Networking*, 2022, pp. 268–281.

[36] F. Zhang, Z. Chang, J. Xiong, J. Ma, J. Ni, W. Zhang, B. Jin, and D. Zhang, "Embracing consumer-level uwb-equipped devices for fine-grained wireless sensing," *Proceedings of the ACM on Interactive, Mobile, Wearable and Ubiquitous Technologies*, vol. 6, no. 4, pp. 1–27, 2023.

[37] T. Zheng, Z. Chen, C. Cai, J. Luo, and X. Zhang, "V2ifi: In-vehicle vital sign monitoring via compact rf sensing," *Proceedings of the ACM on Interactive, Mobile, Wearable and Ubiquitous Technologies*, vol. 4, no. 2, pp. 1–27, 2020.

[38] Z. Chen, T. Zheng, C. Cai, and J. Luo, "Movi-fi: motion-robust vital signs waveform recovery via deep interpreted rf sensing," in *Proceedings of the 27th Annual International Conference on Mobile Computing and Networking*, 2021, pp. 392–405.

[39] Z. Wang, B. Jin, F. Zhang, S. Li, and J. Ma, "Uwb-enabled sensing for fast and effortless blood pressure monitoring," *Proceedings of the ACM on Interactive, Mobile, Wearable and Ubiquitous Technologies*, vol. 8, no. 2, pp. 1–26, 2024.

[40] (2023) Qorvo qm33120w. [Online]. Available: https://www.qorvo.com/products/p/QM33120W

[41] (2023) Murata type2bp. [Online]. Available: https://www.murata.com/en-us/products/connectivitymodule/ultra-wide-band/nxp/type2bp